The young open cluster NGC 2129

Giovanni Carraro,[1,2,3⋆] Brian Chaboyer[4⋆] and James Perencevich[4]

[1]*Departamento de Astronomía, Universidad de Chile, Casilla 36-D, Santiago, Chile*
[2]*Astronomy Department, Yale University, PO Box 208101, New Haven, CT 06520-8101, USA*
[3]*Dipartimento di Astronomia, Università di Padova, Vicolo Osservatorio 2, I-35122 Padova, Italy*
[4]*Department of Physics and Astronomy, Dartmouth College, 6127 Wilder Laboratory, Hanover, NH 03755-3528, USA*

ABSTRACT

The first charge-coupled device $UBV(RI)_{\rm C}$ photometric study in the area of the doubtful open cluster NGC 2129 is presented. Photometry of a field offset 15 arcmin northwards is also provided, to probe the Galactic disc population towards the cluster. Using star counts, proper motions from the UCAC2 catalogue, colour–magnitude and colour–colour diagrams, we demonstrate that NGC 2129 is a young open cluster. The cluster radius is 2.5 arcmin, and across this region we find evidence of significant differential reddening, although the reddening law seems to be normal towards its direction. Updated estimates of the cluster fundamental parameters are provided. The mean reddening is found to be $E(B-V) = 0.80 \pm 0.08$ and the distance modulus is $(m-M)_0 = 11.70 \pm 0.30$. Hence, NGC 2129 is located at 2.2 ± 0.2 kpc from the Sun inside the Local spiral arm. The age derived from 37 photometrically selected members is estimated to be approximately 10 Myr. These stars are used to provide new estimates of the cluster absolute proper-motion components.

Key words: Hertzsprung–Russell (HR) diagram – open clusters and associations: general – open clusters and associations: individual: NGC 2129.

1 INTRODUCTION

NGC 2129 (OCL 467, C0558+233) with $\alpha = 06^{\rm h}01\overset{\rm m}{.}1, \delta = +23^\circ 19\overset{'}{.}3$ and $l = 186\overset{\circ}{.}61, b = +0\overset{\circ}{.}11$, J2000.0) is a clustering of stars located in the Gemini constellation, about 2 degrees south-west of the more conspicuous open clusters M35 and NGC 2158 towards the Galactic anticentre. According to Trumpler (1930) the cluster is moderately concentrated, has a wide range in star brightness, and is relatively rich (class II3m).

The group is dominated (see Fig. 1) by two close bright stars, HD 250289 (LS V +23 15, $V = 8.25$) and HD 250290 (LS V +23 16, $V = 7.36$). Within the errors, these two stars share the same proper motion (Høg et al. 2000) and radial velocity (Liu, Janes & Bania 1989). HD 250289 has $\mu_\alpha \cos\delta = 0.8 \pm 1.2$ (mas yr^{-1}), $\mu_\delta = -1.3 \pm 1.1$ (mas yr^{-1}) and $V_{\rm r} = 17.7 \pm 1.0$ (km s^{-1}); while HD 250290 has $\mu_\alpha \cos\delta = 0.3 \pm 1.2$ (mas yr^{-1}), $\mu_\delta = -1.1 \pm 1.0$ (mas yr^{-1}) and $V_{\rm r} = 17.5 \pm 4.0$ (km s^{-1}). Therefore these two stars probably constitute a pair, and are the two brightest members of the clustering.

The first study of NGC 2129 was performed by Cuffey (1938), who obtained photographic photometry of 111 stars and concluded that this group of stars is a cluster with a diameter of about 5 arcmin located 570 pc from the Sun. He suggested that the two bright stars are members of the system, owing to the concentration of faint stars about them (see Fig. 1). Hoag et al. (1961) and Johnson et al. (1961) obtained and analysed photoelectric/photographic *UBV* photometry of 45 stars down to $V \approx 16$, concluding that the cluster is characterized by variable extinction across its area, with a mean reddening $E(B-V) = 0.67$ and a distance of 2.1 kpc.

Additional *BV* photographic photometry was secured by Voroshilov (1969) with the same limiting magnitude, and *UBV* photoelectric photometry by Lindgren & Bern (1980, table V). Neither of these studies, however, provided information on the cluster parameters. More recently, Peña & Peniche (1994) performed a Strömgren *ubvyβ* study of 37 stars in the region of NGC 2129 and, based upon star counts, they concluded that there is no star clustering in the direction of NGC 2129. Hence, NGC 2129 might simply be a chance alignment of a few bright stars and not a true star cluster.

To clarify this issue, we obtained deep charge-coupled device (CCD) *UBVRI* photometry of a field centred on NGC 2129, and CCD *BVRI* photometry of a control field 15 arcmin away. The size of our fields (about 8 arcmin^2) allows us to cover the entire cluster region (see Fig. 1).

The paper is organized as follows. Section 2 describes the data acquisition and reduction procedure. In Section 3 we compare our

⋆E-mail: gcarraro@das.uchile.cl (GC); brian.chaboyer@dartmouth.edu (BC)

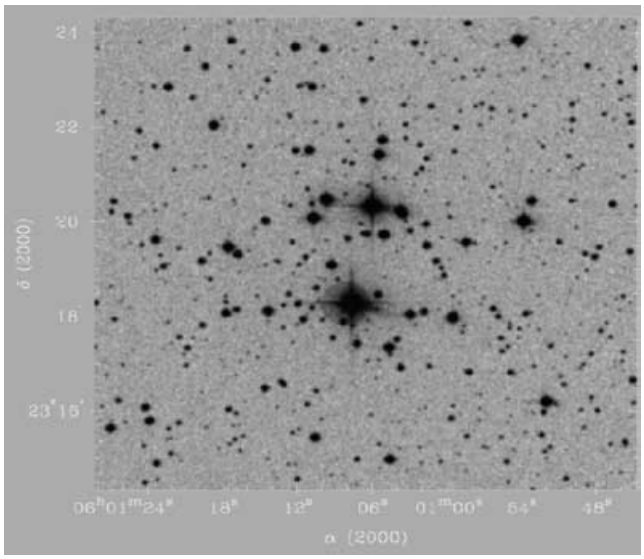

Figure 1. A DSS map of the observed field in the direction of NGC 2129. The size of the field is 9 × 9 arcmin^2. North is up, and east on the left.

photometry to previous studies. Section 4 presents a star count analysis, which is used to determine the cluster size. In Section 5 we discuss NGC 2129 colour–magnitude diagrams (CMDs). An analysis of the cluster reddening and differential absorption is performed in Section 6. Section 7 provides estimates for the cluster age and distance. The basic results of this investigation are highlighted in Section 8.

2 OBSERVATIONS AND DATA REDUCTION

$UBV(RI)_{\rm C}$ photometry of two fields in the region of NGC 2129 were taken at the Michigan–Dartmouth–MIT (MDM) Observatory with the 1.3-m McGraw–Hill telescope on the nights of 2004 February 18 and 19. The comparison field was observed only on the first night, while the cluster field was observed in a similar manner on both nights. The pixel scale of the 1024 × 1024 Templeton CCD is 0.50 arcsec, leading to a field of view of 8.5 × 8.5 arcmin^2 in the sky. The nights were photometric, with an average seeing of 1.4 arcsec. We took several short (4–12 s), medium (40–120 s) and long (400–1200 s) exposures in all the filters to avoid saturation of the brightest stars. None the less, the two bright stars HD 250289 and 250290 were saturated in all exposures, and we used the photoelectric photometry from Hoag et al. (1961) for these two stars.

The data have been reduced with the IRAF[1] packages CCDRED, DAOPHOT, ALLSTAR and PHOTCAL using the point spread function (PSF) method (Stetson 1987). Calibration was secured by the observation of the Landolt (1992) standard fields PG 1047, PG 0231, SA 101 and Rubin 149 for a total of 50 standard stars each night. The two nights turned out to be photometrically very similar, and therefore we decided to use all of the standard stars in a single photometric solution. The calibration equations have the following form:

$$\begin{aligned}
u &= U + (4.419 \pm 0.017) + (0.46 \pm 0.02)X \\
&\quad + (0.118 \pm 0.026)(U - B), \\
b &= B + (2.410 \pm 0.008) + (0.25 \pm 0.02)X \\
&\quad + (0.037 \pm 0.010)(B - V), \\
v &= V + (2.279 \pm 0.007) + (0.16 \pm 0.01)X \\
&\quad - (0.009 \pm 0.009)(B - V), \\
r &= R + (2.429 \pm 0.009) + (0.09 \pm 0.01)X \\
&\quad + (0.061 \pm 0.010)(V - R), \\
i &= I + (3.277 \pm 0.008) + (0.07 \pm 0.01)X \\
&\quad + (0.000 \pm 0.009)(V - I),
\end{aligned}$$

and the final rms of the calibration was 0.020 mag for all the passbands except for U, which had an rms of 0.045 mag. The standard stars have the colour coverage $-1.1 \leqslant (U - B) \leqslant 1.4$, $-0.4 \leqslant (B - V) \leqslant 1.6$, $-0.2 \leqslant (V - R) \leqslant 1.11$ and $-0.3 \leqslant (V - I) \leqslant 2.3$.

Photometric errors have been estimated following Patat & Carraro (2001). Stars brighter than $V \approx 20$ mag have global (internal from DAOPHOT plus calibration) photometric errors lower than 0.15 mag in magnitude and lower than 0.21 mag in colour. The final photometric data (coordinates, U, B, V, R and I magnitudes and errors) consist of about 2500 stars in the cluster field.

The SkyCat tool and the Guide Star Catalogue v2 (GSC-2) at ESO was used to determine an astrometric solution for our photometry and to obtain J2000.0 coordinates for all of the stars. There were approximately 200 stars for which we have both the celestial coordinates on the GSC-2 and the corresponding pixel coordinates from our photometry. Using the IRAF tasks CCXYMATCH, CCMAP and CCTRAN, we find the corresponding transformations between the two coordinate systems and compute the individual celestial coordinates for all the detected stars. The transformations have an rms value of 0.″17, in agreement with other studies (Momany et al. 2001; Carraro et al. 2005).

Important information on the kinematics of the luminous stars in and around our target can be derived from the proper motions available in the UCAC2 catalogue (Zacharias et al. 2004). We retrieved from the catalogue 140 stars located in the same area of our CCD photometry. The result is shown in the vector point diagram of Fig. 2. There is clearly a condensation of stars centred at $\mu_\alpha \cos\delta \simeq 0$ (mas yr^{-1}) and $\mu_\delta \simeq -5$ (mas yr^{-1}), which indicates the presence of a cluster. Recently, Beshenov & Loktin (2004) report for 10 stars

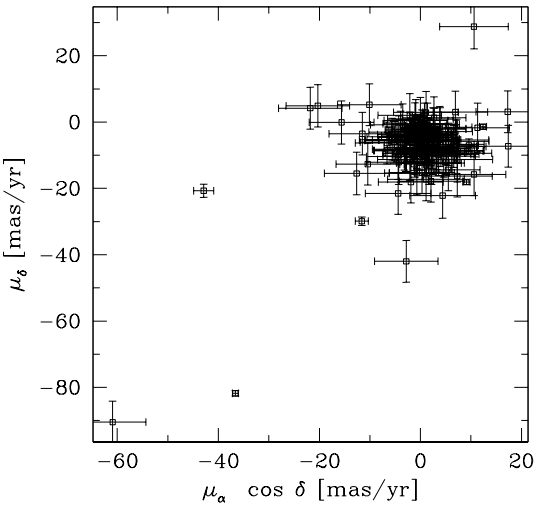

Figure 2. Vector point diagram for all the stars in the field of NGC 2129 from UCAC2.

[1] IRAF is distributed by NOAO, which are operated by AURA under cooperative agreement with the NSF.

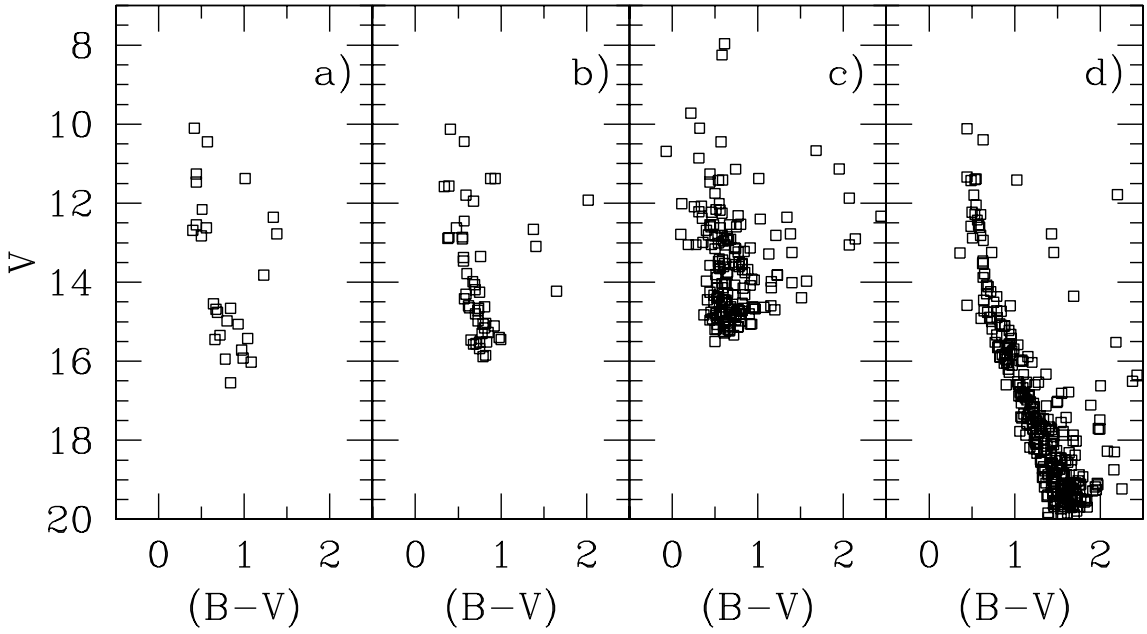

Figure 3. A comparison of the CMD from the present study with those from previous investigations: (a) CMD from Hoag et al. (1961), photoelectric photometry; (b) CMD from Hoag et al. (1961), photographic photometry; (c) CMD from Voroshilov (1969); and (d) CMD from present study, which only includes stars with a colour error less than 0.07 mag.

in NGC 2129 the value $\mu_\alpha \cos\delta = -0.71 \pm 0.28$ (mas yr^{-1}) and $\mu_\delta = -1.53 \pm 0.19$ (mas yr^{-1}) from Tycho 2. A new estimate of the cluster mean proper motion, based upon a new, larger sample of confirmed cluster stars, will be presented in Section 8.

3 COMPARISON WITH PREVIOUS STUDIES

Our CCD investigation is a considerable improvement over previous studies in the region of NGC 2129. In Fig. 3 we compare the CMDs from various authors with ours in the V versus $(B - V)$ plane. As noted before, the two bright stars HD 250289 and 250290 are missed in our CCD photometry since they were saturated. The photometry by Hoag et al. (1961) (panels a and b) is clearly of much better quality than the Voroshilov (1969) photometry (panel c). The main sequence (MS) is narrow in the Hoag et al. (1961) photometry and nicely compares with the present study (panel d). For this reason we took the photometry of two bright stars from this work. The CMD in panel (c) does not present any distinctive feature, and from this alone one might conclude that we are viewing simply a Galactic disc field. We note that the photometry from Cuffey (1938) was the deepest before the present study, although the quality of the photographic magnitudes and colours (which are not in the standard Johnson photometric system) is poor (see Cuffey 1938, fig. 9).

We performed a comparison on a star-by-star basis with the photoelectric photometry of Hoag et al. (1961) and found from 16 stars in common:

$$V_{\rm H} - V_{\rm CC} = -0.04 \pm 0.05,$$
$$(B - V)_{\rm H} - (B - V)_{\rm CC} = -0.03 \pm 0.06,$$
$$(U - B)_{\rm H} - (U - B)_{\rm CC} = 0.10 \pm 0.13,$$

where the suffix H stands for Hoag et al. (1961), and CC for the present paper. A comparison to the Hoag et al. (1961) photographic photometry (61 common stars) yields

$$V_{\rm H} - V_{\rm CC} = -0.07 \pm 0.11,$$
$$(B - V)_{\rm H} - (B - V)_{\rm CC} = -0.04 \pm 0.09,$$
$$(U - B)_{\rm H} - (U - B)_{\rm CC} = 0.01 \pm 0.23.$$

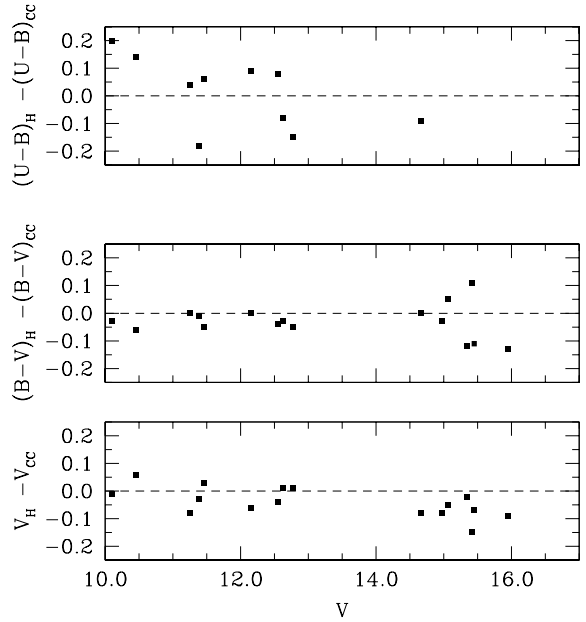

Figure 4. Comparison between our photometry and the photoelectric photometry by Hoag et al. (1961).

These comparisons are shown in Figs 4 and 5. The photoelectric photometry agrees well with our photometry to $V = 12.5$, but fainter than this magnitude some scatter starts to be present (Fig. 4). There appear to be systematic offsets between the data sets in Fig. 5, although the sizes of the differences are reasonable in a comparison between CCD and photographic photometry. Finally, we notice that there appears to be a colour term effect in the U band, which runs in opposite directions in the photoelectric (Fig. 4) and photographic (Fig. 5) photometry.

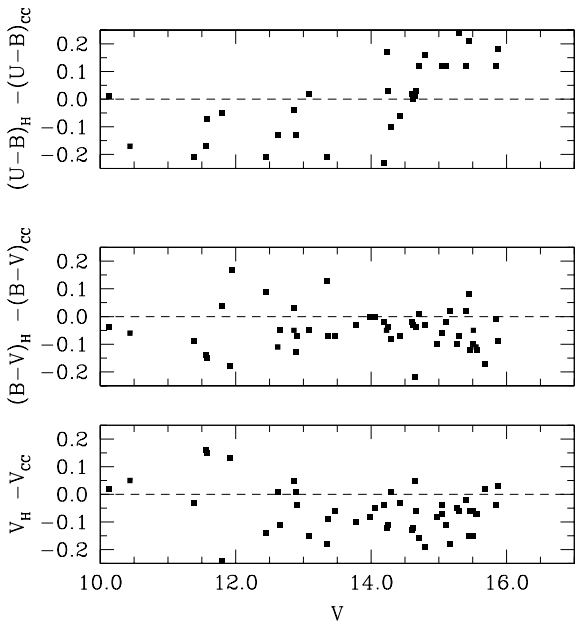

Figure 5. Comparison between our photometry and the photographic photometry by Hoag et al. (1961).

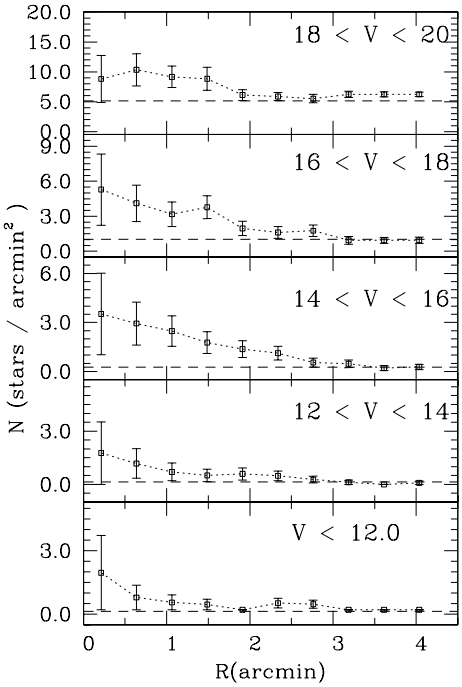

Figure 6. Star counts as a function of radius from the adopted cluster centre for various magnitude intervals. The dashed line in each panel indicates the mean density level of the surrounding Galactic disc field at that magnitude level.

4 STAR COUNTS AND CLUSTER SIZE

The cluster radius is one of the most important cluster parameters, useful, together with cluster mass, for a determination of cluster dynamical parameters. The aim of this section is to obtain the surface density distribution of NGC 2129, and to derive the cluster size by means of star counts. Star counts allow us to determine statistical properties of clusters with respect to the surrounding stellar background.

In Fig. 1, NGC 2129 appears as a concentration of bright stars in a region of about 4 arcmin diameter. To derive the radial stellar surface density, we determine the highest peak in the stellar density to find the cluster centre. The two bright stars HD 250289 and 250290 have been included in this and the following star count calculations. The adopted centre is placed at $\alpha = 06^{\rm h}01^{\rm m}07\overset{\rm s}{.}0$, $\delta = +23^{\circ}19'18\overset{''}{.}0$, similar to that given by Dias et al. (2002).

The radial density profile is constructed by performing star counts inside increasing concentric annuli 0.5 arcmin wide, around the cluster centre and then dividing by their respective surface areas. This is done as a function of apparent magnitude, and compared with the mean density of the surrounding Galactic field in the same brightness interval. The contribution of the field has been estimated through star counts in the region outside 6 arcmin from the cluster centre. Poisson standard deviations have been computed and normalized to the area of each ring as a function of the magnitude, both for the cluster and for the field. The result is shown in Fig. 6, where one readily sees that NGC 2129 emerges significantly from the mean field for magnitudes brighter than $V \approx 18$. At fainter magnitudes the cluster starts to mix with the Galactic disc population. Based on the radial density profiles in Fig. 6, we find that stars brighter than $V = 20$ provide a cluster radius of approximately 2 arcmin. We adopt as a final estimate of the radius 2.0 ± 0.5 arcmin. This value of the cluster radius is adopted throughout this work and is in basic agreement with the estimate of 2.5 arcmin reported by Cuffey (1938), which was simply based on visual inspection. We stress, however, that this radius is not the limiting radius of the cluster, but the distance from the cluster centre at which the cluster population starts to be confused with the field population. At odds with Peña & Peniche (1994), we find that NGC 2129 appears as a clear star cluster standing above the mean Galactic field.

5 ANALYSIS OF THE CMDs

Further confirmation of the cluster nature of NGC 2129 can be found in the comparison of the CMD for the cluster and the control field region depicted in Fig. 7. In this figure we show the V versus $(V-I)$ and V versus $(V-R)$ CMDs of NGC 2129 stars within 2.5 arcmin from the cluster centre, and the same CMDs for stars in a similar area region taken from the control field. We considered only stars brighter than $V = 21$ and with $\sigma_V \leqslant 0.05$. It is readily seen that the cluster actually exists, and it exhibits a nice MS extending from $V = 10$ down to $V = 21$. On the other hand, the field MS sharply stops at $V \approx 17.5$, and contains only a handful of brighter stars. The cluster MS presents some scatter, larger than expected from the sole photometric errors (see Section 2), and which we ascribe mostly to differential reddening across the cluster area (see next section). This is not unexpected, as a result of the cluster position, low in the Galactic thin disc.

6 INDIVIDUAL REDDENINGS, MEMBERSHIP AND DIFFERENTIAL REDDENING

We use *UBV* photometry to derive the stars' individual reddenings and membership. Briefly, individual reddening values have been computed by means of the usual reddening free parameter Q:

$$Q = (U-B) - 0.72(B-V) - 0.05(B-V)^2,$$

and the distribution of the stars in the two-colour diagram. We follow the procedure described in Carraro (2002), Ortolani et al. (2002)

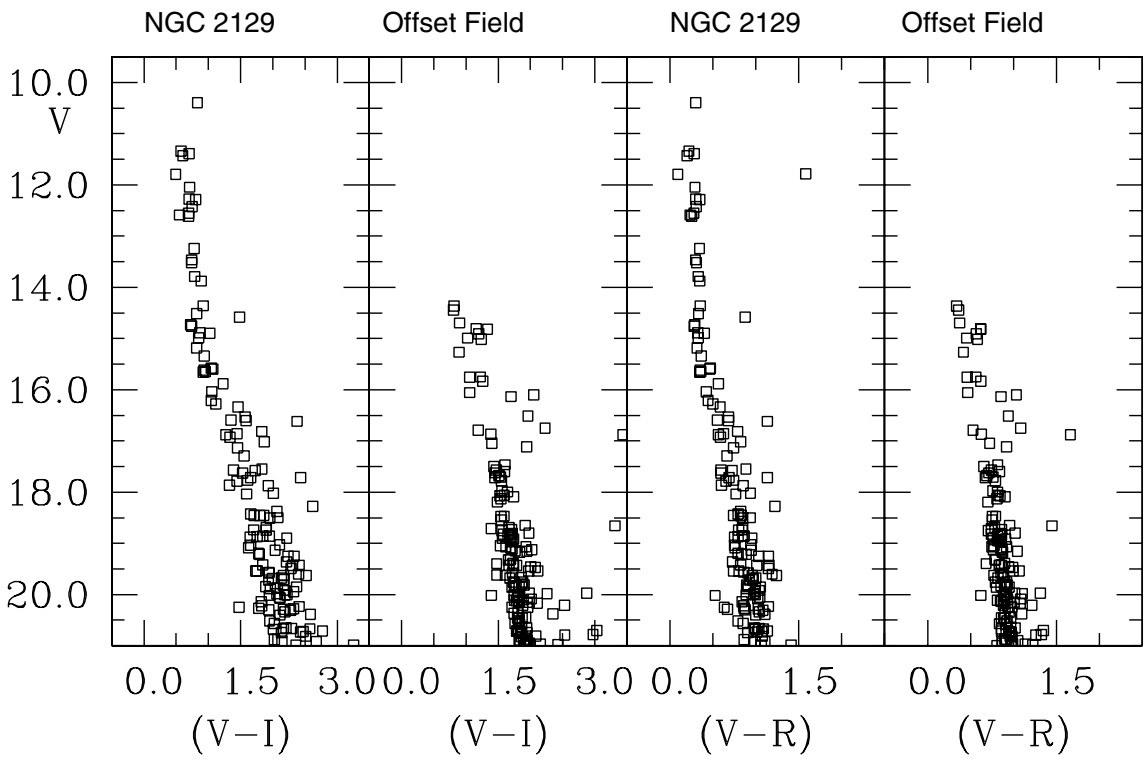

Figure 7. CMDs for the stars in the field of NGC 2129 and in the offset field.

and Baume, Vazquez & Carraro (2005), where the young open clusters Trumpler 15, NGC 1220 and Markarian 50 were studied. This method is a powerful one to isolate early spectral type (from O to A5) stars having common reddening, which are most probably cluster members [see also, for a reference, the study of Trumpler 14 by Vazquez et al. (1996)]. Note that the reddening-based membership selection gives similar results to proper-motion-based membership selection [see Cudworth, Martin & DeGioia-Eastwood (1993) and Patat & Carraro (2001) for some applications to star clusters in the Carina region].

Our results are shown in Fig. 8, where we plot all the stars brighter than $V = 19$ having *UBV* photometry in the two-colour diagram. In this plot the solid line is an empirical zero-age main sequence (ZAMS) taken from Schmidt-Kaler (1982). The bulk of the stars are confined within a region defined by two ZAMS shifted by $E(B-V) = 0.60$ and 0.90 (dashed lines), respectively. The 37 stars (filled symbols) that occupy this region have a mean reddening $E(B-V) = 0.80 \pm 0.08$ (rms). Since the spread in reddening is larger than the photometric errors, which are typically $\Delta(U-B) \approx \Delta(B-V) \approx 0.03$, this indicates the presence of differential reddening across the cluster, as suggested also by Cuffey (1938). This technique has been applied to all the stars except for HD 250289 and 250290, which are stars with spectral type B2IIIe and B3I (Morgan, Code & Whitford 1955; Hoag & Applequist 1965) and are probably evolved stars. For these two stars, absolute magnitudes and colours have been derived from Wegner (1994), assuming their spectral types and luminosity classes.

For some stars, an unambiguous reddening solution is not possible, and these stars are plotted with open symbols. A reddening solution is not possible since these stars are located in a region where larger reddening ZAMS cross the $E(B-V) = 0.90$ mag ZAMS, making it impossible to effectively disentangle members from non-members.

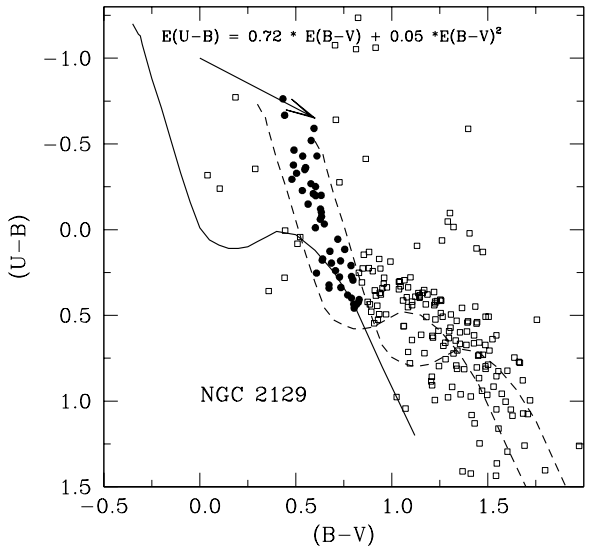

Figure 8. The *UBV* colour–colour diagram for all the stars in the field of NGC 2129 having *UBV* photometry. The solid line is the Schmidt-Kaler (1982) empirical ZAMS, whereas the dashed lines are the same ZAMS, but shifted by $E(B-V) = 0.60$ and 0.90, respectively. Filled symbols indicate stars having reddening in the range $0.60 \leqslant E(B-V) \leqslant 0.90$, for which an unambiguous reddening solution has been possible.

In summary, there are 37 photometric members, for which we can derive estimates of the distance and age of the cluster. The member stars are listed in Table 1, together with coordinates, magnitudes, colours and proper-motion component from UCAC2. We derived the photometric spectral type from the Q parameter (columns 10 and 11 in Table 1). These spectral types compare very well with

Table 1. Basic data of photometric likely member stars in the field of NGC 2129.

ID	Hoag et al.(1961)	RA	DEC	V	$(B-V)$	$(U-B)$	$(V-R)$	$(V-I)$	E$(B-V)$	Q	*Sp. Type*	μ_α	μ_δ
2	3	6:00:53.77	+23:19:58.14	10.115	0.442	-0.516	0.245	0.528	0.707	-0.844	B0-B1	0.0±0.9	-2.3±0.7
3	4	6:01:03.66	+23:20:14.24	11.391	0.547	-0.351	0.283	0.721	0.812	-0.760	B2	-0.8±1.0	-1.7±0.9
4	7	6:01:05.25	+23:21:24.85	11.431	0.490	-0.463	0.198	0.603	0.779	-0.829	B1	0.2±1.0	-7.6±0.6
5		6:01:17.50	+23:19:30.80	11.400	0.535	-0.429	0.200	0.649	0.824	-0.839	B1	0.8±6.5	-0.6±6.3
7		6:01:04.81	+23:17:20.00	11.794	0.523	0.042	0.090	0.493	0.649	-0.347	B7	4.4±6.5	22.2±6.8
8		6:01:05.00	+23:19:43.51	12.043	0.551	-0.362	0.291	0.710	0.821	-0.774	B2	-1.7±3.7	-2.1±1.4
10		6:01:03.04	+23:18:02.17	12.277	0.534	-0.227	0.299	0.703	0.755	-0.627	B3	3.9±6.4	-2.9±7.2
11		6:01:09.26	+23:19:06.21	12.286	0.603	-0.198	0.345	0.801	0.832	-0.652	B3	0.6±1.0	-1.0±0.8
12	8	6:01:14.43	+23:18:08.68	12.224	0.504	-0.329	0.253	0.631	0.751	-0.705	B2	-0.7±1.4	1.2±0.8
13		6:01:03.46	+23:20:09.15	12.426	0.563	-0.149	0.306	0.747	0.765	-0.571	B4	-2.5±2.6	-2.4±1.3
14	10	6:00:58.45	+23:19:32.38	12.586	0.488	-0.376	0.233	0.553	0.747	-0.740	B2	1.1±0.6	-2.5±0.6
15	11	6:01:04.94	+23:21:43.33	12.614	0.591	-0.210	0.254	0.695	0.820	-0.653	B3	0.8±6.3	-9.5±6.3
16		6:01:10.84	+23:21:31.74	12.552	0.578	-0.267	0.278	0.690	0.824	-0.701	B2	2.7±6.3	1.3±6.3
17		6:01:10.88	+23:15:28.03	12.884	0.509	0.082	0.262	0.659	0.619	-0.298	B8	-1.3±1.9	-1.0±1.9
18		6:01:17.80	+23:18:07.07	12.941	0.634	-0.075	0.339	0.866	0.829	-0.552	B4	-0.6±1.8	-2.9±1.8
19		6:01:11.77	+23:23:42.82	12.810	0.601	-0.010	0.253	0.673	0.766	-0.462	B5	-0.6±1.8	-5.5±1.3
22		6:01:07.35	+23:17:26.27	13.515	0.632	-0.199	0.308	0.740	0.868	-0.675	B3	-10.1±6.3	5.2±6.3
23		6:01:05.64	+23:18:28.03	13.242	0.732	0.182	0.344	0.777	0.867	-0.372	B7	-1.7±1.9	-1.6±1.9
24		6:01:01.59	+23:19:29.59	13.461	0.628	-0.121	0.296	0.737	0.838	-0.594	B3	0.2±2.0	-4.6±2.0
26		6:01:08.42	+23:17:53.81	13.876	0.633	-0.102	0.345	0.890	0.837	-0.578	B4	-1.3±1.9	-1.0±1.9
28		6:01:09.50	+23:23:39.74	13.529	0.627	-0.059	0.289	0.748	0.816	-0.532	B4	0.2±2.0	-4.6±2.0
29		6:01:01.92	+23:18:05.37	13.787	0.648	-0.032	0.327	0.787	0.833	-0.521	B4	0.6±0.6	-1.3±0.6
32		6:01:19.67	+23:19:13.17	14.068	0.672	0.341	0.196	0.762	0.738	-0.166	B9	-1.1±1.9	-5.9±1.9
33		6:01:14.82	+23:16:31.43	14.234	0.718	0.056	0.334	0.894	0.892	-0.487	B5	-12.6±6.4	-15.5±6.4
36		6:01:19.06	+23:23:19.70	14.290	0.672	0.321	0.250	0.750	0.744	-0.185	B9	2.7±6.3	1.3±6.3
40		6:00:46.60	+23:20:18.04	14.449	0.638	0.178	0.323	0.706	0.749	-0.302	B8	1.1±0.6	-2.5±0.6
47	17	6:01:01.58	+23:19:55.78	14.760	0.686	0.194	0.282	0.741	0.804	-0.323	B8	-1.1±6.3	-10.2±6.4
48		6:01:12.02	+23:18:17.04	14.886	0.707	0.238	0.324	0.865	0.816	-0.296	B8	2.7±6.3	1.3±6.3
53		6:00:44.46	+23:23:09.40	14.919	0.607	0.253	0.294	0.632	0.685	-0.203	B9	-4.4±6.5	-21.5±6.3
54		6:01:00.86	+23:19:09.02	14.727	0.640	0.170	0.287	0.726	0.754	-0.312	B8	7.2±6.3	-5.4±6.3
55		6:01:07.89	+23:19:39.38	14.987	0.728	0.276	0.329	0.847	0.830	-0.275	B8	1.7±6.4	-12.4±6.4
60		6:01:02.89	+23:19:47.88	15.179	0.734	0.336	0.315	0.819	0.818	-0.219	B9	-1.7±3.7	-2.1±1.4
66	22	6:01:11.31	+23:19:16.47	15.336	0.790	0.399	0.366	0.933	0.867	-0.201	B9	0.6±0.6	-1.3±0.6
70	24	6:01:00.96	+23:22:24.99	15.518	0.770	0.381	0.345	0.857	0.848	-0.203	B9	-1.1±1.9	-5.9±1.9
79		6:01:10.51	+23:18:37.43	15.643	0.801	0.434	0.360	0.954	0.870	-0.175	A0.5	-0.2±6.4	-4.2±6.3
82		6:01:09.29	+23:17:34.05	15.619	0.816	0.437	0.354	0.934	0.887	-0.184	A0.5	3.9±6.4	-2.9±7.2

what we can found in the literature. In fact, Hoag & Applequist (1965) report for stars 3, 4 and 7 spectral types of B3III, B6 and B5, very close to our determinations. In addition, McCuskey (1967) found that the seven brightest stars in the field of NGC 2129 are of OB spectral type, and Chargeishvili (1988) reported for a few bright stars spectral classification from an objective prism analysis, suggesting that they are of B spectral type.

In Fig. 9 we plot all the stars having *UBV* photometry in the $(V-I)$ versus $(B-V)$ diagram. In this plot the solid line is the normal reddening vector from Dean, Warren & Cousins (1978), whereas the dotted and dashed lines are the intrinsic positions for stars of luminosity classes V and II, respectively, taken from Cousins (1978a,b). Given that the stars follow the standard reddening vector, the ratio of total to selective absorption, $R_V = A_V/E(B-V)$, is basically normal.

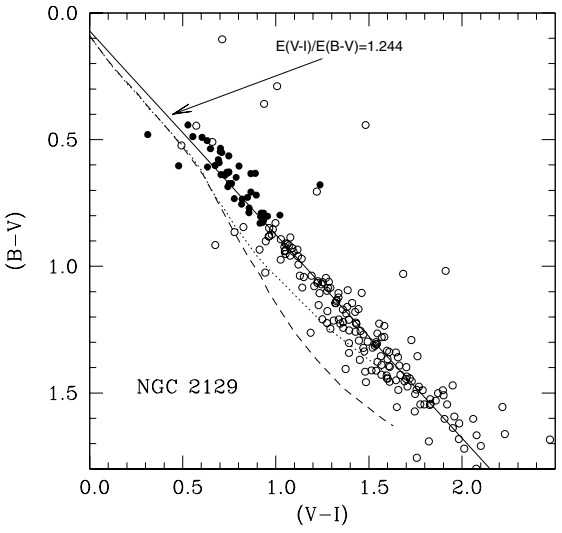

Figure 9. The *BVI* colour–colour diagram for all the stars in the field of NGC 2129 having *UBV* photometry. The solid line is the normal reddening vector, whereas the dotted and dashed lines are the intrinsic positions for stars of luminosity classes V and II, respectively, taken from Cousins (1978a,b). Only stars for which an unambiguous reddening solution has been possible are plotted. Symbols are as in Fig. 8.

7 AGE AND DISTANCE

The reddening-corrected CMDs for the likely member stars from Table 1 are plotted in Fig. 10. We have superposed the empirical Schmidt-Kaler (1982) ZAMS (solid line), shifted by $(m-M)_0 = 11.7 \pm 0.2$ mag, which provides a nice fit to the observed distribution of stars. A 0.70 mag brighter ZAMS (dashed line) is shown to mimic the location of unresolved binary stars. The two brightest stars

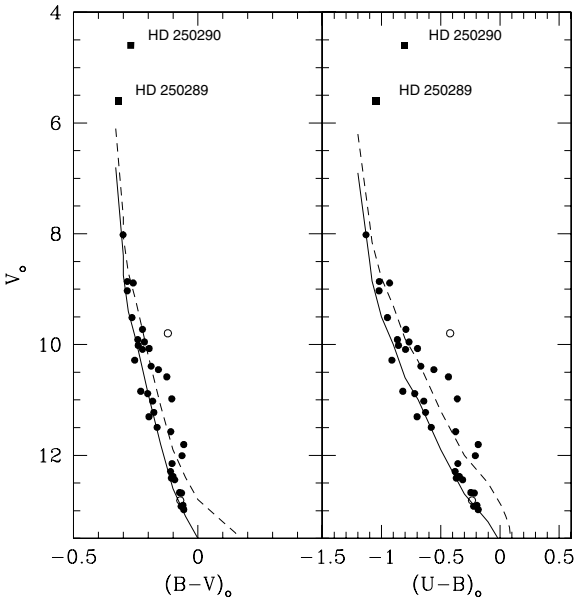

Figure 10. Reddening-corrected CMDs for NGC 2129. Superposed is an empirical ZAMS taken from (solid line Schmidt-Kaler 1982) shifted by $(m - M)_{0,V} = 11.70$. The dashed line is the same ZAMS 0.70 mag brighter, which mimics the position of unresolved binary stars.

HD 250289 and 250290 are plotted as solid squares. The open circle is a star (number 9) that was found to be a photometric member, but whose proper-motion components differ significantly from the mean. Therefore, we consider it as a foreground star. Its position in the CMDs supports this conclusion.

The absolute distance modulus implies that NGC 2129 is located 2200 ± 200 pc from the Sun. The relatively large uncertainty is due to the difficulty of fitting the almost vertical structure of the MS. The Galactocentric coordinates are $X = -250$ pc, $Y = 2200$ pc, $Z = 4$ pc, and the Galactocentric distance is $R_{\rm GC} = 10.70$ kpc. The cluster lies in the extension of the Local spiral arm towards the Galactic Third Quadrant. The distance modulus we find is in nice agreement with Johnson et al. (1961), who found $(m - M)_0 = 11.60$ and a distance of 2100 pc.

The two brightest stars HD 250289 and 250290 are of spectral type B2III and B3I and are likely to be evolved stars. On the other hand, the star at $V \approx 8.1$ appears to be on the main sequence with an absolute magnitude of $M_V = -3.6$, and an estimated spectral type of approximately B2–B3. The two-colour diagram (Fig. 8) enables one to estimate the spectral classification of stars with spectral types ranging from B2 to A5 (see Table 1). If the stars having B2–B3 spectral type are still along the MS, we infer that the age of NGC 2129 is around 10 Myr.

8 CONCLUSIONS

In this paper we have presented the first CCD multicolour photometry for the stars in the field of NGC 2129, and provide the first estimate of its fundamental parameters. Our findings can be summarized as follows:

(i) NGC 2129 is a compact group of stars with a radius of 2.0–2.5 arcmin, or 1.0–1.3 pc at the distance of the cluster.

(ii) We identified 37 likely members with spectral type earlier than A5 on the basis of reddening, proper motion and the position in the reddening-corrected CMDs.

(iii) The cluster is situated about 2200 pc away from the Sun in the anticentre direction, inside the Local spiral arm.

(iv) The mean reddening is $E(B - V) = 0.82 \pm 0.08$, and there is substantial differential reddening.

(v) The probable age of NGC 2129 is approximately 10 Myr.

(vi) The mean proper motion components of the 37 cluster members are $\mu_\alpha \cos\delta = 1.03 \pm 0.52$ (mas yr^{-1}) and $\mu_\delta = -3.32 \pm 0.90$ (mas yr^{-1}).

ACKNOWLEDGMENTS

GC is profoundly indebted to Brian Skiff for providing numerous very useful comments and suggestions. The work of GC is supported by Fundación Andes. This research was supported in part by an NSF Career grant 0094231 to BC. BC is a Cottrell Scholar of the Research Corporation.

REFERENCES

Baume G., Vazquez R. A., Carraro G., 2005, MNRAS, 355, 475
Beshenov G. V., Loktin A. V., 2004, Astron. Astrophys. Trans., 23, 103
Carraro G., 2002, MNRAS, 331, 785
Carraro G., Baume G., Piotto G., Mendez R. A., Schmidtobreick L., 2005, A&A, 436, 527
Chargeishvili K. B., 1988, Abastumanskaia Astrof. Obs. Bul., 65, 3
Cousins A. W. J., 1978a, Mon. Notes Astron. Soc. S. Afr., 37, 62
Cousins A. W. J., 1978b, Mon. Notes Astron. Soc. S. Afr., 37, 77
Cudworth K. M., Martin S. C., DeGioia-Eastwood K., 1993, AJ, 105, 1822
Cuffey J., 1938, Ann. Harv. Coll. Obs., 106, 39
Dean J. F., Warren P. R., Cousins A. W. J., 1978, MNRAS, 183, 569
Dias W. S., Alessi B. S., Moitinho A., Lepine J. R. D., 2002, A&A, 389, 871
Hoag A. A., Applequist L., 1965, ApJS, 12, 215
Hoag A. A., Iriarte B., Mitchell R. I., Hallam K. L., Sharpless S., 1961, Publ. US Naval Obs., 17, 347
Høg E. et al., 2000, A&A, 355, L27
Johnson H. L., Hoag A. A., Johnson H. L., Iriarte B., Mitchell R. I., Hallam K. L., 1961, Lowell Obs. Bull., 113 (8), 133
Landolt A. U., 1992, AJ, 104, 340
Lindgren H., Bern K., 1980, A&AS, 42, 335
Liu T., Janes K. A., Bania T. M., 1989, AJ, 98, 626
McCuskey S. W., 1967, AJ, 72, 1199
Momany Y. et al., 2001, A&A, 379, 436
Morgan W. W., Code A. D., Whitford A. E., 1955, ApJS, 2, 41
Ortolani S., Carraro G., Covino S., Bica E., Barbuy B., 2002, A&A, 391, 179
Patat F., Carraro G., 2001, MNRAS, 325, 1591
Peña J. H., Peniche R., 1994, Rev. Mex. Astron. Astrophys., 28, 139
Schmidt-Kaler Th., 1982, in Schaifers K., Voigt H. H., eds, Numerical Data and Functional Relationships in Science and Technology, Landolt-Börnstein, New Series, Group VI, Vol. 2(b). Springer, Berlin, p. 14
Stetson P. B., 1987, PASP, 99, 191
Trumpler R., 1930, Lowell Obs. Bull., 14, 171
Vazquez R. A., Baume G., Feinstein A., Prado P., 1996, A&AS, 116, 75
Voroshilov V. I., 1969, Publ. Kiev Univ.
Wegner W., 1994, MNRAS, 270, 229
Zacharias N., Urban S. E., Zacharias M. I., Wycoff G. L., Hall D. M., Money D. G., Rafferty T.J., 2004, AJ, 127, 3043

This paper has been typeset from a TEX/LATEX file prepared by the author.